Observation of the Limiter *H* Mode in the JT-60 Tokamak with Lower-Hybrid Current Drive

S. Tsuji, K. Ushigusa, Y. Ikeda, T. Imai, T. Itami, M. Nemoto, K. Nagashima, Y. Koide, Y. Kawano, T. Fukuda, T. Kondoh, M. Shimada, H. Nakamura, O. Naito, H. Yoshida, T. Nishitani, H. Kubo, K. Tobita, Y. Kusama, S. Ishida, M. Sato, N. Isei, T. Sugie, N. Miya, R. Yoshino, K. Uehara, and JT-60 Team

Japan Atomic Energy Research Institute, Naka Fusion Research Establishment, Naka-machi, Naka-gun, Ibaraki-ken 311-01, Japan

(Received 20 November 1989)

The *H* mode was achieved in limiter discharges of a tokamak with lower-hybrid current drive for the first time. Simultaneous application of rf powers at two different frequencies such as 1.74 and 2.23 GHz or 1.74 and 2.0 GHz appeared to be effective in the attainment of the *H* mode. The threshold lower-hybrid power was as low as the Ohmic-heating power with hydrogen plasmas. A nearly steady-state edge-localized-mode-free *H* mode with a duration up to 3.3 sec was established without significant impurity accumulation.

PACS numbers: 52.55.Fa, 52.35.Hr, 52.55.Pi

Since the discovery of a phase of improved confinement during neutral-beam-injection (NBI) heating, known as the *H* mode, in the poloidal divertor configuration of ASDEX,[1] the *H* mode has been obtained with several heating schemes such as ion-cyclotron-resonance heating (ICRH),[2-4] a combination of NBI and electron-cyclotron heating (ECH),[5] ECH,[6,7] and Ohmic heating alone.[8] The *H* mode has also been realized in limiter discharges.[3,9,10] This Letter reports the first observation of the *H* mode in limiter discharges with lower-hybrid current drive (LHCD). We observed sharp *L*-to-*H* and *H*-to-*L* transitions in distinction from the particle-confinement improvement during LHCD in Versator II.[11] The threshold LH power of the *H*-mode transition was about 1.2 MW with hydrogen plasmas.

In JT-60, the *H* mode was obtained in the outer or lower divertor configuration with NBI heating and combined heating with NBI and ICRH or NBI and LH.[12] The threshold heating power was about 16 MW. In contrast to the beam-heated *H* mode with frequent edge localized modes (ELM) in the divertor configuration, the limiter *H* mode with LHCD produced ELM-free *H* phases longer than 3 sec.

Typical plasmas of the present experiments had $R=3.04$ m, $a=0.89$ m, and nearly circular cross section which contacted inner bumper-type limiters. The gap between the outermost flux surface and the outside limiters was about 5 cm. Graphite first walls were conditioned by Taylor-type discharge cleaning. The plasma was developed from hydrogen gas at $B_t=4.5$ T, and the plasma current was 1.5 MA resulting in $q_{sur}\sim 4.7$. The LH power was applied from two launchers; a conventional grill of 8 (torroidal) × 4 (poloidal) and a multijunction type of 24×4 phased-array wave guides.[13,14] The launchers were located at the outer (low field) side of the torus at an upward angle of 40° from the midplane. Most of the experiments were conducted with LH waves at two different frequencies of 1.74 and 2.23 GHz from the multijunction and conventional launchers, respectively. The phase differences between adjacent wave guides were 180° and 90°, the phasing of which provides high directivity for current drive. The peaks of the refractive index parallel to the magnetic field were about 2.1 and 1.5, respectively.

Typical traces of an *H*-mode discharge with LHCD are shown in Fig. 1. The LH power of about 1.4 MW was launched for 3 sec. The gas feed was turned off just

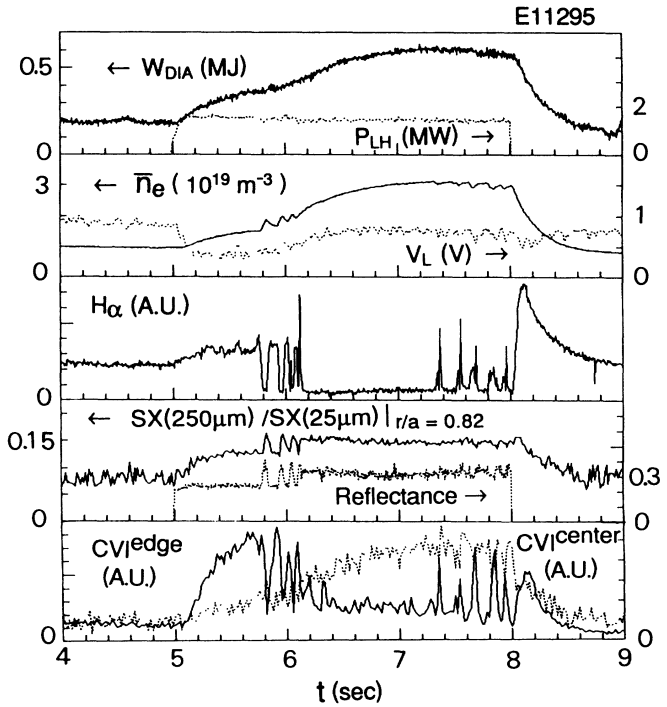

FIG. 1. Time evolution of plasma stored energy evaluated by diamagnetics, injected LH power, line-averaged electron density, one-turn loop voltage, H_α emission, ratio of soft-x-ray signals through Be foils, reflection coefficient of the conventional launcher, and CVI line signals along chords near the edge ($r/a\sim 0.9$) and through the center.

before the application of the LH pulse. The L-mode plasma of this discharge lasted for 0.7 sec before the first H transition was triggered at 5.76 sec. After repeated short H phases, the discharge entered a quiescent H phase at 6.2 sec. A sharp drop in H_α emission below the Ohmic level was accompanied by increases in the plasma stored energy and in the line-averaged electron density. All H_α signals fell almost the same way as the H_α trace in the figure along a view chord just above the plasma-limiter interaction points. The low-energy neutral-flux levels decreased substantially as well. This behavior indicates a sudden improvement in the global particle confinement. Roughly speaking, the improvement is by an order of magnitude since the electron density was nearly doubled with reduced particle recycling by a factor of about 5. The loop voltage increased gradually since the fraction of current driven by the LH waves was reduced due to the rise of the electron density. The impurity accumulation, which is often observed during ELM-free H phases, was so modest that the discharge reached a quasisteady state. Although the dominant impurity ions were carbon, the carbon influx behaved almost the same way as hydrogen. The giant ELM's were accompanied by carbon influx as seen in the $(\mathrm{C\,VI})^{\mathrm{edge}}$ trace.

The formation of the electron-temperature pedestal was confirmed by filtering of soft-x-ray emission near the edge with Be foils of 250- and 25-μm thickness; sharp rises in the ratio of the two signals were detected at the H transitions as shown in the second box from the bottom of Fig. 1. The T_e profile measured by an eight-point Thomson-scattering system remained almost the same both in magnitude and in shape despite the increasing density. Temperature changes at the edge were not clear within error bars. The peakedness parameter of the electron-density profile, $n_e(0)/\langle n_e\rangle$, calculated from the Thomson data changed from about 1.9 during the L-mode phase to about 1.5 just after the H transition. Then it increased slightly during the H-mode phase to around 1.7. A preliminary measurement by a millimeter-wave reflectometer suggested steepening of the edge density profile at the H transitions. These observations agree with the characteristic signatures of the H mode.

It should be noted that the LH power could be coupled to the H-mode plasma. The sudden variation of the edge plasma parameters, however, modified the rf coupling to the plasma. The reflection coefficient of the power from the conventional launcher increased by about 0.1 at the H transitions as shown in Fig. 1, whereas it changed only a few percent for the multijunction type.

The operational region where the H mode was observed is illustrated in Fig. 2 in terms of the line-averaged electron density and LH power for the combination of 1.74 and 2.23 GHz. The lines indicate the electron-density intervals which evolved during each LH pulse. The solid and open lines indicate that the discharge stayed in the L phase and in the quiescent H phase, respectively. The broken lines correspond to the marginal intervals where short H phases were repeated as in the period from 5.8 to 6.1 sec in Fig. 1. Figure 2 shows that the threshold LH power is around 1.2 MW and that there is a lower limit for the electron density of about 2×10^{19} m^{-3} to achieve the H mode. The H mode was reproducible as long as the LH power and the electron density exceeded the thresholds.

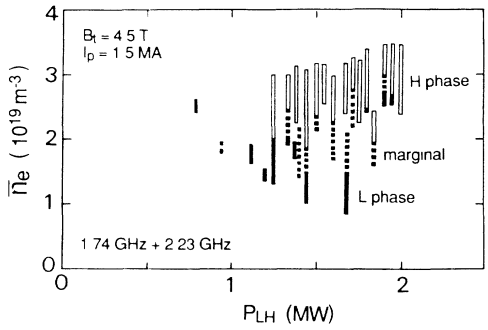

FIG. 2. Electron-density region where the H-mode phase was observed as a function of LH power. Broken lines represent marginal intervals where short H phases were repeated.

The open lines in Fig. 2 represent the increment in the electron density with the H mode without gas feed. Then the electron density stayed nearly constant presumably because the LH power does not provide particle fueling like NBI. A gas puff of 2 Pa m^3/sec for 0.5-sec duration into an H-mode phase did not destroy the H mode despite inducing frequent ELM's. The volume-averaged electron density increased later on by about 6×10^{18} m^{-3} which corresponds to twice the usual fueling efficiency of about 0.3. When the gas feed was kept during the LH pulse, however, the H transition tended to be delayed until the gas was turned off.

By feedback controlling the electron density at the LH initiation to be above the threshold density, we could lengthen the H-mode phase up to 4.6 sec. Figure 3 shows a discharge where the ELM-free H-mode phase lasted for 3.3 sec. The gap between the outermost flux surface and the outside limiters was controlled to be about 6 cm since only short H phases were triggered when it was less than 4 cm. This sensitive gap dependence of the H-mode quality is common to the beam-heated H mode in diverted plasmas.[15]

The Z_{eff} value estimated from visible bremsstrahlung emission and the n_e and T_e profiles from Thomson-scattering measurements increased slightly from about four during the L phase to around five at the later phase of the H mode. The soft-x-ray emission profile became slightly peaked with time, which suggested impurity accumulation at the center. Nevertheless, the radiation power measured by bolometer arrays remained abut 40%

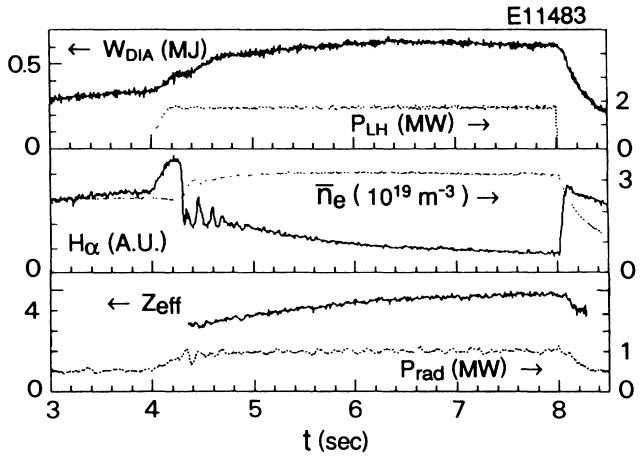

FIG. 3. Time histories from a discharge with ELM-free phase of 3.3 sec. Traces are the same as in Fig. 1 except the bottom box; effective ionic charge from visible bremsstrahlung emission and total radiation power.

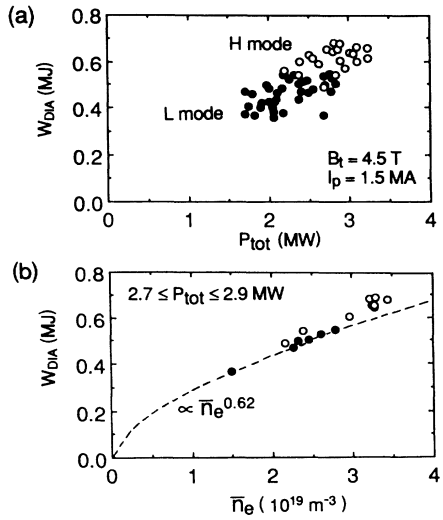

FIG. 4. (a) Plasma stored energy as a function of $P_{tot}=P_{Oh}+P_{LH}$. Open and solid circles represent data from the H and L mode, respectively. (b) Electron-density dependence of plasma stored energy when the total power is restricted. The curve shows a dependence as $\propto n_e^{0.62}$.

of the total input power as shown in Fig. 3. The attainment of the modest impurity accumulation even in the ELM-free phase may be due to the relatively low input power.

The properties of energy confinement are summarized in Fig. 4. The plasma stored energy increases almost linearly with the total input power as shown in Fig. 4(a). Here we assumed that the injected LH power was completely absorbed by the plasma. The scatter of the data points is mainly due to the variation of the electron density. The energy confinement is enhanced by up to 30% by the H mode. The increment in the plasma stored energy, however, is primarily gained by the increase in the electron density as plotted in Fig. 4(b). The L-mode plasmas with LHCD have almost the same electron-density dependence as the Ohmic stored energy[16] of $W_{Oh} \propto n_e^{0.62}$ presumably because the total input power does not greatly exceed the Ohmic input. Although the difference is small, the H-mode data points appear to have a little stronger n_e dependence than Ohmic.

The critical factor in obtaining the H mode with LHCD is not yet established. The effect of the current-profile modification by LHCD on the H transition is not clear since the change in the internal inductance was small. Other heating schemes such as NBI or ICRH using the second-harmonic resonance with powers up to 20 and 2 MW, respectively, never produced the limiter H mode in JT-60. The application of LH power at two different frequencies, however, appeared to be favorable in the attainment of the H mode. When the frequencies from the two launchers were both set at 1.74 GHz, no H mode was observed within applied powers up to 1.5 MW. Although the combined LH power at 2.0 GHz of higher than 2.0 MW produced the H mode, the H phase did not last long due to abruptly enhanced carbon influx.

The beat frequency for 2.23 and 1.74 GHz is 490 MHz, for which the seventh-harmonic ion-cyclotron resonance occurs at the plasma center and the ninth at the outer edge when B_t =4.5 T. The H transition became obscure with lowering B_t down to 3.5 T. In the combination of 1.74 and 2.0 GHz, sharp H transitions were triggered in the range of B_t from 2.8 to 4.3 T; the beat frequency corresponds to from the third to the eighth harmonic in the plasma column. The waves at the beat frequencies, however, were not detected by a rf probe. Thus it is not clear whether the presence of the ion-cyclotron harmonic resonances is connected with the H transition.

NBI heating was combined to examine the effect of wave-particle interactions. Figure 5 shows an example where an NB power of 1.2 MW was injected to an H-mode phase. The beam pulse interrupted the H phase as seen in the concurrent rise in the H_α emission and fall in the electron density. Note that the trace of the electron-cyclotron emission (ECE) at $1.5\omega_{ce}$ multiplied by n_e, which is a measure of the LH coupling to fast electrons,[17] dropped at the same time. Hard-x-ray emission behaved similarly to $I_{ECE}(1.5\omega_{ce})\times n_e$. During the L phase with NBI, beam acceleration by the LH waves[18] was observed in the neutral flux as shown in Fig. 5(b). These facts suggest that the H mode could not be sustained when the LH power was absorbed by beam ions.

Such ion tails were not observed in the H phase with LH alone. No parametric decay instabilities were observed either. Nonthermal ECE spectra suggest a favorable effect of fast electrons on the H transition. In fact, ECH has been reported to be more efficient than NBI in producing the H mode.[6-8] The presence of fast electrons

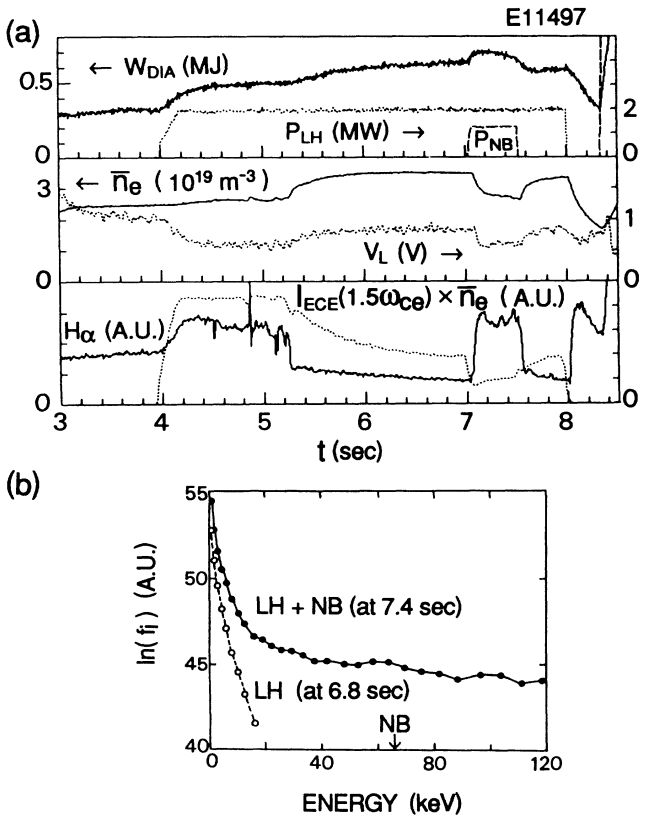

FIG. 5. (a) Time evolution of a discharge where the H mode with LHCD was destroyed by NBI. (b) Neutral-particle spectra from a charge-exchange analyzer whose chord normal to the magnetic field crosses the NB line at the plasma center. NB injection energy is indicated by an arrow.

may be relevant to the low threshold power.

It is a puzzling question that the H mode with LHCD has never been obtained in the lower X-point divertor configuration. One of the possible causes is that gas feed must be maintained to keep the electron density above the threshold against the divertor pumping. The favorable effect of the application of LH powers at two different frequencies is left for future work. Resolving these issues should shed light on the H-mode physics.

In summary, the mode with LHCD was demonstrated in the limiter discharges of JT-60. These discharges exhibited the characteristics of the H mode. The improvement in particle confinement was prominent. The ELM-free H phase with durations up to 3.3 sec was attained without significant impurity accumulation.

The authors wish to thank the members of the Japan Atomic Energy Research Institute, who have contributed to the JT-60 project throughout its progress. Dr. M. Yoshikawa and Dr. M. Tanaka are gratefully thanked for continued support and encouragement. The authors also appreciate fruitful discussions with Dr. K. Itoh and Dr. S. I. Itoh.

[1]F. Wagner *et al.*, Phys. Rev. Lett. **49**, 1408 (1982).
[2]K. Steinmetz *et al.*, Phys. Rev. Lett. **58**, 124 (1987).
[3]H. Matsumoto *et al.*, Nucl. Fusion **27**, 1181 (1987).
[4]B. J. D. Tubbing *et al.*, Nucl. Fusion **29**, 1953 (1989).
[5]K. Hoshino *et al.*, Nucl. Fusion **28**, 301 (1988).
[6]J. Lohr *et al.*, Phys. Rev. Lett. **60**, 2630 (1988).
[7]K. Hoshino *et al.*, Phys. Rev. Lett. **63**, 770 (1989).
[8]K. H. Burrel *et al.*, in *Proceedings of the Twelfth International Conference on Plasma Physics and Controlled Nuclear Fusion Research, Nice, France, 1988* (International Atomic Energy Agency, Vienna, 1989), paper CN-50/A-III-4.
[9]J. Manickam *et al.*, in *Proceedings of the Twelfth International Conference on Plasma Physics and Controlled Nuclear Fusion Research, Nice, France, 1988* (Ref. 8), paper CN-50/A-VII-4.
[10]K. Toi *et al.* (to be published).
[11]S. C. Luckhardt *et al.*, Phys. Fluids **29**, 1985 (1986).
[12]H. Nakamura *et al.* (to be published).
[13]T. Imai *et al.*, Nucl. Fusion **28**, 1341 (1988).
[14]Y. Ikeda *et al.*, Nucl. Fusion **29**, 1815 (1989).
[15]M. Keilhacker *et al.*, in *Proceedings of the Twelfth International Conference on Plasma Physics and Controlled Nuclear Fusion Research, Nice, France, 1988* (Ref. 8), paper CN-50/A-III-2.
[16]M. Kikuchi *et al.*, Nucl. Fusion **27**, 1239 (1987).
[17]K. Ushigusa *et al.*, Nucl. Fusion **29**, 265 (1989).
[18]T. Imai *et al.*, Nucl. Fusion **30**, 161 (1990).